Atmos. Chem. Phys. Discuss., 13, 14447–14475, 2013
www.atmos-chem-phys-discuss.net/13/14447/2013/
doi:10.5194/acpd-13-14447-2013

Atmospheric Chemistry and Physics Discussions

A parameterisation for the activation of cloud drops including the effects of semi-volatile organics

P. J. Connolly[1], **D. O. Topping**[1], **F. Malavelle**[2], **and G. McFiggans**[1]

[1]School of Earth, Atmospheric and Environmental Sciences, The University of Manchester, Manchester, UK
[2]Department of Mathematics, University of Exeter, Exeter, UK

Received: 3 May 2013 – Accepted: 10 May 2013 – Published: 3 June 2013

Correspondence to: P. J. Connolly (p.connolly@man.ac.uk)

Published by Copernicus Publications on behalf of the European Geosciences Union.

Abstract

We present a parameterisation of aerosol activation, including co-condensation of semi-volatile organics, for warm clouds that has applications in large-scale numerical models. The scheme is based on previously developed parameterisations that are in the literature, but has two main modifications. The first is that the total aerosol mass is modified by the condensation of organic vapours entering cloud-base, whereas the second is that this addition of mass acts to modify the median diameter and the geometric standard deviation of the aerosol size distribution. It is found that the scheme is consistent with parcel model calculations of co-condensation under different regimes. Such a parameterisation may find use in evaluating important feedbacks in climate models.

1 Introduction

The mean global radiative forcing associated with the indirect effect of aerosols on clouds is currently the most uncertain of those assessed by the Intergovernmental Panel on Climate Change (IPCC) (Soloman et al., 2007), having an uncertainty that is approximately the size of the total net anthropogenic radiative forcing. Increasing aerosol concentrations, possibly by anthropogenic activity, affects the radiative properties of stratocumulus (Sc) clouds by increasing the number of cloud drops in them, which increases the scattering of short-wave radiation (Twomey, 1977) and extends the lifetime of the cloud (Albrecht, 1989). This is thought to result in a cooling effect of approximately $-0.7\,\mathrm{W\,m^{-2}}$ globally.

Topping and McFiggans (2012) showed through calculation of the equilibrium between organic vapours and water vapour on pre-existing non-volatile aerosol that the organic vapour may act to significantly alter the non-volatile aerosol's ability to act as Cloud Condensation Nuclei (CCN). Topping et al. (2013) confirmed this effect and quantified it under different aerosol and updraft regimes by performing detailed parcel

ACPD
13, 14447–14475, 2013

model calculations of the diffusion of organic and water vapours to an aerosol population and assessed the effect this has on the activation of aerosol into cloud drops.

Kulmala et al. (2004) explain that such an effect may manifest as an important climate feedback mechanism, similar to that proposed by Charlson et al. (1987); however, the full "bin-microphysics" treatment used by Topping et al. (2013) is too computationally expensive for use within General Circulation Models (GCMs), which are the main tools used to calculate radiative forcing and climate feedbacks. The computational expense is also true for other large-scale atmospheric models. Hence, so that the effect proposed by Kulmala et al. may be assessed, our aim for this paper was to derive and test a parameterisation that captures the effect of semi-volatile co-condensation of organic vapours on the resulting number of cloud droplets.

Various parameterisation schemes to determine the number of cloud droplets in warm clouds have been developed and used in General Circulation Model (GCM)s. Two similar schemes are those proposed by Abdul-Razzak et al. (1998) and also by Fountoukis and Nenes (2005), which have been developed further since the original papers to include additional effects. These schemes have been shown to perform well (Ghan et al., 2011) and since they are physically-based there is the opportunity to develop them further to include the process that is the focus of this paper.

2 Description of methodology

The methodology that has been adopted in this paper is based on cloud activation schemes currently in the scientific literature. Namely, the schemes by Abdul-Razzak et al. (1998) and the later scheme by Fountoukis and Nenes (2005). A brief overview of both of these schemes is given here to provide the backdrop for the additions that we have made to include the effect of semi-volatile co-condensation.

ACPD
13, 14447–14475, 2013

2.1 Basic scheme without co-condensation

In formulating the scheme for activation the assumption of an adiabatic parcel rising through an atmosphere in hydrostatic balance is made.

Central to both the above schemes is the assumption that the aerosol size distribution is distributed lognormally with respect to size:

$$n_{\mathrm{ap}}\left(d_{\mathrm{ap}}\right) = \frac{N_{\mathrm{ap}}}{\sqrt{2\pi}\ln\sigma}\exp\left[-\frac{\ln^2\left(d_{\mathrm{ap}}/d_{\mathrm{m}}\right)}{2\ln^2\sigma}\right] \tag{1}$$

where n_{ap} is the number of aerosols per unit volume, per logarithmic interval; d_{ap} is the particle diameter; $\ln\sigma$ is the standard deviation of $\ln\frac{d_{\mathrm{ap}}}{d_{\mathrm{m}}}$; d_{m} is the median diameter and N_{ap} is the total number of particles per unit volume. Both schemes introduce a change of variable, $S_{\mathrm{crit}} = \frac{2}{\sqrt{B}}\left(\frac{2A}{3d_{\mathrm{ap}}}\right)^{3/2}$, to Eq. (1) to give:

$$n_{\mathrm{ap}}\left(S_{\mathrm{crit}}\right) = \frac{2N_{\mathrm{ap}}}{3S_{\mathrm{crit}}\sqrt{2\pi}\ln\sigma}\exp\left[-\frac{\ln^2\left(\left[S_{\mathrm{c,\,m}}/S_{\mathrm{crit}}\right]^{(2/3)}\right)}{2\ln^2\sigma}\right] \tag{2}$$

where $S_{\mathrm{c,\,m}}$ is the critical supersaturation of an aerosol with diameter equal to d_{m} and S_{crit} is the critical supersaturation of an aerosol, diameter d_{ap}. The supersaturation, S_{l} is given by $S_{\mathrm{l}} = \frac{(e-e_{\mathrm{sat,\,l}})}{e_{\mathrm{sat,\,l}}}$ so the rate of change is (quotient rule):

$$\frac{\mathrm{d}S_{\mathrm{l}}}{\mathrm{d}t} = \frac{1}{e_{\mathrm{sat,\,l}}}\frac{\mathrm{d}e}{\mathrm{d}t} - \frac{e}{e^2_{\mathrm{sat,\,l}}}\frac{\mathrm{d}e_{\mathrm{sat,\,l}}}{\mathrm{d}t} \tag{3}$$

From the definition of vapour mixing ratio $w_{\mathrm{l}} = \frac{\epsilon e}{P}$ we make e the subject ($e = \frac{w_{\mathrm{l}}P}{\epsilon}$) and define the rate of change of vapour pressure (via product rule) for insertion into Eq. (3):

ACPD
13, 14447–14475, 2013

$$\frac{de}{dt} = \frac{1}{\epsilon} P \frac{dw_v}{dt} + \frac{1}{\epsilon} w_v \frac{dP}{dt} \tag{4}$$

For the second term on the right of Eq. (3) we make use of the Clausius–Clapyeron equation ($\frac{de_{sat,\,l}}{dT} = \frac{L_v e_{sat}}{R_v T^2}$):

$$\frac{de_{sat,\,l}}{dt} = \frac{de_{sat,\,l}}{dT}\frac{dT}{dt} = \frac{L_v e_{sat}}{R_v T^2}\frac{dT}{dt} \tag{5}$$

The rate of change of temperature can be expressed in terms of the rate of change of pressure and and phase of water via the 1st law of thermodynamics (time derivative):

$$c_p \frac{dT}{dt} - R_a \frac{T}{P}\frac{dP}{dt} - L_v \frac{dw_l}{dt} - L_s \frac{dw_i}{dt} = 0 \tag{6}$$

Therefore we substitute Eq. (6) into Eq. (5) and substitute the result and Eq. (4) into Eq. (3), resulting in:

$$\frac{dS_l}{dt} = \frac{1}{e_{sat,\,l}}\left(\frac{1}{\epsilon} P \frac{dw_v}{dt} + \frac{1}{\epsilon} w_v \frac{dP}{dt}\right) - \frac{e}{e_{sat,\,l}}\frac{L_v}{R_v T^2}\left(\frac{R_a T}{c_p P}\frac{dP}{dt} + \frac{L_v}{c_p}\frac{dw_l}{dt} + \frac{L_s}{c_p}\frac{dw_i}{dt}\right) \tag{7}$$

Noting that Eq. (7) depends on the rate-of-change of pressure we take the time derivative of the hydrostatic relation for the parcel:

$$\frac{dP}{dt} = -\frac{gP}{R_a T} w \tag{8}$$

(where w is the vertical wind speed) and substitute Eq. (8) into Eq. (7):

$$\frac{dS_l}{dt} = (S_l + 1)\left[\left(\frac{g}{c_p} - \frac{g}{R_a T}\right) w - \left(\frac{1}{w_v} + \frac{L_v^2}{R_v T^2 c_p}\right)\frac{dw_l}{dt} - \cancel{\left(\frac{1}{w_v} + \frac{L_v L_s}{R_v T^2 c_p}\right)\frac{dw_i}{dt}}\right] \tag{9}$$

ACPD
13, 14447–14475, 2013

where we have also used the fact that total water in the parcel is conserved and have neglected the ice phase:

$$\frac{\mathrm{d}w_\mathrm{v}}{\mathrm{d}t} + \frac{\mathrm{d}w_\mathrm{l}}{\mathrm{d}t} + \cancel{\frac{\mathrm{d}w_\mathrm{i}}{\mathrm{d}t}} = 0$$

For cloud droplet activation it is the peak in S_l that is important in determining how many aerosol are activated into cloud drops. The peak in supersaturation is the stationary point of Eq. (9), which is located at $\frac{\mathrm{d}S_\mathrm{l}}{\mathrm{d}t} = 0$:

$$0 = \left(\frac{g}{c_p} - \frac{g}{R_\mathrm{a}T}\right) w - \left(\frac{1}{w_\mathrm{v}} + \frac{L_\mathrm{v}^2}{R_\mathrm{v}T^2 c_p}\right) \frac{\mathrm{d}w_\mathrm{l}}{\mathrm{d}t} \tag{10}$$

The quantity $\frac{\mathrm{d}w_\mathrm{l}}{\mathrm{d}t}$ is dependent on the supersaturation and how it varies in time up to the supersaturation peak. The reason for this is that the supersaturation time history determines the size of the droplets, which requires an integral to be evaluated, and the size of the droplets determines the instantaneous rate of change of supersaturation. Both Abdul-Razzak et al. (1998) and Fountoukis and Nenes (2005) schemes define different forms of the integral to be evaluated; however, both depend on the peak in supersaturation and the properties of the aerosol particle size distribution.

The mass growth rates of drops is described by a growth equation first derived by Maxwell:

$$\frac{\mathrm{d}m}{\mathrm{d}t} \cong 2\pi d G \rho_\mathrm{w} S_\mathrm{l} \tag{11}$$

where d is the diameter of a drop and G is a thermodynamic factor. Diameter growth rates follow a quadratic law found by making the change of variable $m = \frac{\pi}{6} d^3 \rho_\mathrm{w}$ to Eq. (11) and integrating:

$$\frac{\mathrm{d}d}{\mathrm{d}t} = \frac{G S_\mathrm{l}}{d} \tag{12}$$

ACPD
13, 14447–14475, 2013

which yields:

$$\mathrm{d}(t)^2 = d_{\mathrm{crit}}^2 + 2G \int_{\tau=S_{\mathrm{crit}}}^{t(S_{\mathrm{max}})} S_{\mathrm{l}}(t')\mathrm{d}t' \tag{13}$$

where τ is the time at which the critical supersaturation is reached.

To find $\frac{\mathrm{d}w_{\mathrm{l}}}{\mathrm{d}t}$ at the critical supersaturation in Eqs. (10, 13) is substituted into Eq. (11), which is multiplied by Eq. (2) and integrated between 0 and S_{max}. This yields:

$$\frac{\mathrm{d}w_{\mathrm{l}}}{\mathrm{d}t} = 2\pi\rho_{\mathrm{w}}GS_{\mathrm{l}} \int_0^{S_{\mathrm{l}}} \left[\mathrm{d}(S')^2 + 2G \int_{S'}^{t(S_{\mathrm{max}})} S(t')\mathrm{d}t' \right]^{1/2} n_{\mathrm{ap}}(S')\mathrm{d}S' \tag{14}$$

The difference between the Abdul-Razzak et al. (1998) and the Fountoukis and Nenes (2005) schemes are in the estimation of Eq. (14). Abdul-Razzak et al. (1998) neglect a term in the integral and use an approximation for the lower bound by Twomey (1959) to formulate an analytical expression, which is dependent on S_{max}. This is then substituted into Eq. (10) and rearranged for S_{max}. Fountoukis and Nenes (2005), assume that the aerosol size distribution consist of two populations, one of swollen aerosol and one of activated aerosol. They also approximate the integral, but in such a way that S_{max} cannot be isolated when substituted into Eq. (10), and hence S_{max} is found by iteration. For details the reader is directed to the respective papers.

2.2 Inclusion of co-condensation in the parameterisation

A simple modification that can be made to either of the above schemes to take account of condensed semi-volatile vapours during activation is to alter the Köhler curve parameters (such as the aerosol density, van't Hoff factors and molecular masses) and the size distribution parameters (N_{ap}, $\ln\sigma$ and d_{m}) so that the total aerosol mass is equal

ACPD
13, 14447–14475, 2013

to the non-volatile aerosol mass and the mass of condensed organics. Total aerosol particle number concentration is unaffected by condensation so the variables that may be changed are the geometric standard deviation and the median diameter of the distribution. Once these parameters have been found either of the two schemes can be adopted as is to calculate the activated fraction.

2.2.1 Determining the amount of condensed organic vapour

To a first approximation we may neglect curvature in the calculation of condensed organic vapour, mainly because at the point of activation many of the aerosols are swollen to large sizes as they take up water. Calculations by Topping et al. (2013) showed that in all cases considered at cloud base, for the volatility distribution presented by Cappa and Jimenez (2010), the vast majority of organic vapour is in the condensed phase. This may not be true for the most volatile organic components in the atmosphere, but was the case for the range of vapour pressures measured by Cappa and Jimenez (2010).

An accurate calculation of the amount of each organic component that is in the condensed phase may be achieved by use of the molar based partitioning model for secondary organic aerosol (McFiggans et al., 2010). However, as we only consider components with a saturation concentration, C^*, less than $1000\,\mu g\,m^{-3}$ we make the assumption that all semi-volatile organics condense at cloud base. In order to test to accuracy of this assumption we repeated some of the parcel model calculations by Topping et al. (2013), but using an initial non-volatile aerosol distribution of ammonium sulphate that was distributed lognormally in size. The geometric standard deviation, $\ln\sigma$, and the median diameter, d_m, were set to 0.5 and 60 nm respectively, while four different simulations were performed for different total aerosol number concentrations, $N = [10, 100, 500, 1000]\,cm^{-3}$.

The results show that, for updraft speeds that are lower than those typically found in trade-wind Cumulus (Cu) clouds (see Sect. 3.3), the assumption that all organic vapour condenses at cloud base is a reasonable approximation for aerosol concen-

ACPD
13, 14447–14475, 2013

trations higher than $\sim 100\,cm^{-3}$. Figure 1a shows the amount of organic vapour in the simulation as a function of temperature for a constant updraft speed of $0.1\,m\,s^{-1}$. Here, cloud base is situated around 292.1 K and it can be seen that almost all of the organic vapour condenses onto the aerosol size distribution as it enters cloud. Figure 1b shows the same except for an updraft speed of $2.0\,m\,s^{-1}$. In this plot it is seen that the lower aerosol concentrations result in less condensation by virtue of there being less competition for the organic vapours, and the finite time required for vapour diffusion. For aerosol concentrations higher than $500\,cm^{-3}$ it is still seen that most of the organic compounds are in the condensed phase. Thus, at high updraft speeds and low aerosol concentrations it appears that the assumption of all of the organic being the in condensed phase is an overestimate. However, at these high updraft speeds and low aerosol concentrations, nearly all of the aerosol will act as Cloud Condensation Nuclei (CCN) in any case, without the need for additional semi-volatiles; hence, the validity of this assumption needs to be evaluated within the parameterisation as a whole. This is done in Sect. 3.

2.2.2 Altering the lognormal distribution

The addition of organic material to the aerosol size distribution adds mass to the total aerosol burden, but does not alter the number of aerosol particles. This has the effect of increasing the median diameter, d_m, and altering the geometric standard deviation, $\ln\sigma$. The constraint of total aerosol mass (a single constraint) is insufficient to determine both d_m and $\ln\sigma$ (two parameters) so a method to close the parameterisation was sought. To investigate ways of doing this we first used the parcel model described by Topping et al. (2013) to investigate how the geometric standard deviation changed following co-condensation of organic vapour.

The non-volatile aerosol distribution and the aerosol size distribution following co-condensation (note this is the effective aerosol distribution without the associated water) are shown in Fig. 2, which shows that the geometric standard deviation decreases

ACPD
13, 14447–14475, 2013

substantially following the condensation of organic vapours. The green dashed lines on the plot show the original non-volatile aerosol particle distribution, but shifted to the right by a constant factor. This shows that there is good agreement between the shape of a non-volatile aerosol particle distribution, that is shifted by a constant along the diameter axis, and the final distribution. This therefore implies that the arithmetic standard deviation of the aerosol particle distribution is approximately invariant before and after condensation of the organic vapours. This is demonstrated in Fig. 3, where the same aerosol distributions are plotted on a linear diameter axis. The appendix provides arguments as to why the arithmetic standard deviation of the "dry" aerosol distribution does not change following co-condensation.

In order to determine how the geometric standard deviation changed we used the definition of the arithmetic standard deviation, s.d., of a lognormal distribution (see http://en.wikipedia.org/wiki/Log-normal_distribution):

$$\text{s.d.} = \exp\left(\ln d_\text{m} + \frac{1}{2}\ln^2\sigma\right)\sqrt{\exp\left(\ln^2\sigma\right) - 1} \tag{15}$$

Equation (15), with the assumption that s.d. stays the same before and after co-condensation, allows us to calculate the geometric standard deviation after co-condensation; we do this in the following way. Firstly we compute the arithmetic standard deviation for the non-volatile aerosol particle distribution, which becomes the constraint for the distribution after co-condensation. Secondly we compute the new total aerosol mass, m_tot, by assuming that all organics condense onto the aerosol distribution. The density of the aerosol, ρ_ap is assumed to be constant over the whole distribution and is calculated using an appropriate mixing rule:

$$\frac{m_\text{tot}}{\rho_\text{ap}} = \sum_i \frac{m_i}{\rho_i} \tag{16}$$

A root finding method is used to alter the d_m of the aerosol distribution following condensation of the organic vapour, from which the corresponding geometric standard

ACPD
13, 14447–14475, 2013

deviation is calculated by root finding Eq. (15), with s.d. set to the arithmetic standard deviation of the non-volatile aerosol distribution. This is done until the total mass in the aerosol size distribution, found using an expression for the 3rd moment of a lognormal distribution, is equal to m_{tot}. It should be noted that changing the geometric standard deviation in this way is a crucial step in the scheme (see Sect. 3.2).

3 Performance of scheme

3.1 Framework to test scheme

An adiabatic framework was used to test the scheme. That is given an initial RH = 0.95, $T = 293.15$ and $P = 950$ mbar, as well as organic vapour concentrations (taken from Cappa and Jimenez, 2010), we derived the values of T and P at cloud base and applied the parameterisation for those conditions; the calculation of cloud base T and P was as follows. Firstly, the temperature of cloud-base was determined by root-finding the temperature at which the initial water vapour pressure is equal to the saturation vapour pressure. Secondly, the cloud-base pressure was determined by conserving dry potential temperature. Although strictly one should take in to account the effects of moist air on the gas constant and the heat capacity of the air, neglecting this results in very little difference to the calculated cloud-base pressure.

In order to assess the performance of the scheme we compare it against a parcel model with bin-microphysics, which is described by Topping et al. (2013). The parcel model was run for for aerosol lognormal parameters: $\ln\sigma = 0.5$; $d_m = 60$ nm and for $N_{ap} = [10, 100, 500, 1000]\,cm^{-3}$ and run for 8 different updraft velocities: 0.01, 0.1, 0.5, 1.0, 2.0, 5.0, 8.0 and $10.0\,m\,s^{-1}$. This was done for both with and without co-condensation of organic vapours; therefore resulting in a total of 64 simulations to compare with the parameterisation.

ACPD
13, 14447–14475, 2013

3.2 Comparison for different aerosol distributions

To compare the schemes with the parcel model we varied the initial aerosol concentration in the non-volatile aerosol size distribution, looking at total number concentrations ranging from $10\,cm^{-3}$ to $1000\,cm^{-3}$ as described above. We performed calculations using the parameterisation for a range of updraft velocities from 0.01 to $10\,m\,s^{-1}$ both with and without the effect of co-condensation of organic vapour. Figure 4 shows the comparison between the parcel model and the parameterisation implemented via the Abdul-Razzak et al. (1998) scheme. It shows that, while the addition of the co-condensation parameterisation improves the agreement at higher updraft speeds ($w >\sim 0.5\,m\,s^{-1}$) it does not perform very well at lower updraft speeds ($w <\sim 0.5\,m\,s^{-1}$). In fact, the parcel model shows that semi-volatile co-condensation serves to enhance droplet number concentrations across the range of updraft speeds for all choices of N, whereas the parameterisation using the Abdul-Razzak et al. (1998) scheme shows that this is reversed at low updraft speeds. Therefore this implementation of the parameterisation does not do well over the range of updraft speeds chosen for investigation.

Figure 5 shows a similar comparison to Fig. 4, but with the parameterisation implemented using the Fountoukis and Nenes (2005) scheme. This shows that there is no dramatic "cross-over" (where the co-condensation activated fraction goes from being higher to lower than the standard scheme) in the activated fraction for with and without semi-volatile co-condensation. Therefore this implementation of the parameterisation is more consistent with the parcel model. Although it is not a perfect comparison it does show good general agreement over a range of conditions.

In order to demonstrate how important the shifting of the geometric standard deviation is we have compared the parameterisation scheme using the Fountoukis and Nenes (2005) scheme, but without shifting the geometric standard deviation (as described in Sect. 2.2.2). This comparison is shown in Fig. 6 and demonstrates that the reduction in $\ln\sigma$ is a main factor in enhancing the activated fraction. It is evident that

ACPD
13, 14447–14475, 2013

not reducing $\ln\sigma$ results in an underestimation of the activated fraction (compare Fig. 6 to Fig. 5) for all updraft speeds, and this is especially evident when aerosol number concentrations are high.

3.3 Application to model derived updraft PDFs

The purpose of this section is to show how the schemes behave for updraft velocities that are atmospherically relevant. In order to achieve this a cloud-reserving-model (CRM) was used to derive a probability density function (PDF) of the updraft velocity at cloud base for idealised trade wind Cumulus (Cu) based on data from the Rain In Cumulus over the Oceans (RICO) experiment (vanZanten et al., 2011).

The case in question is a shallow, marine Cumulus (Cu) case in the trades over the western Atlantic. The domain size extends over a 256 × 256 horizontal grid with a resolution of 100 m. The vertical grid consists of 100 layers on a stretched grid and uses a spacing of 40 m in the boundary layer, increasing to 100 m in the mid-troposphere up to 7 km. It is then further reduced in resolution to 200 m towards to top of the domain, which is at 10 km. The vertical velocity at grid points entering the cloud base were sampled from the model and are shown in Fig. 7. This shows a mode updraft speed at cloud base of $\sim 0.3\,\mathrm{m\,s^{-1}}$, which is positively skewed, with peak updrafts extending up to around ~ 1.5–$2.0\,\mathrm{m\,s^{-1}}$

We generated a histogram of activated fractions for the probability density function (PDF) of updrafts shown in Fig. 7 by randomly sampling w_{cb} base on its probability of occurrence, using a sample size of 100 000. The activated fraction was calculated using the parameterisation scheme based on either Abdul-Razzak et al. (1998) or Fountoukis and Nenes (2005) for both with and without semi-volatile co-condensation. The non-volatile aerosol size distribution assumed in this comparison was lognormal with $N_{\mathrm{ap}} = 1000\,\mathrm{cm^{-3}}$, $\ln\sigma = 0.5$ and $d_{\mathrm{m}} = 60\,\mathrm{nm}$. Figure 8 shows cumulative frequencies ($n = 10^5$) of the activated fraction for the parcel model runs; the Fountoukis and Nenes implementation of the scheme and the Abdul-Razzak et al. (1998) implementation.

ACPD
13, 14447–14475, 2013

The figure shows that addition of semi-volatile co-condensation broadens the range of activated fractions and importantly leads to a much higher frequency at higher activated fractions (as noted by the fact that the cumulative frequency is close to unity at lower activated fractions).

Relative to the parcel model it is also evident that both parameterisation schemes have higher frequencies at low activated fractions, which is due to them underestimating the activated fractions at low updraft speeds (see Figs. 4 and 5). It is evident that the Abdul-Razzak et al. (1998) implementation of the scheme has a high frequency at activated fractions less than ~ 0.1, which is inconsistent with the parcel model. The reason for this is the rather sharp "cross-over" at low updrafts in Fig. 4, where switching on semi-volatile co-condensation results in less droplets activating in the Abdul-Razzak et al. (1998) scheme, but not in the parcel model. This effect is much less evident in the Fountoukis and Nenes implementation of the scheme (Fig. 8, centre plot).

The over estimation of low activated fractions in the Abdul-Razzak et al. (1998) scheme results in a significant underestimation of the mean activated fraction when semi-volatile co-condensation is switched on (by almost a factor of two), whereas the Fountoukis and Nenes (2005) implementation is much closer to the parcel model.

4 Discussion

In the development of a parameterisation for activation of aerosols that includes the effect of condensation of organics we had to make assumptions for how much of the semi-volatile condenses on to the aerosol at cloud base, following which we used this constraint as a basis for an "equivalent dry" aerosol size distribution to be input into the existing activation schemes. It was found by running a detailed parcel model that, at low updraft speeds, diffusion of the organic vapour to the aerosol was fast enough to stay close to equilibrium. For a typical aerosol size distribution this resulted in almost all of the organic vapour condensing at cloud base. At higher updraft speeds and low total aerosol number concentrations diffusion was too slow and resulted in significant

ACPD
13, 14447–14475, 2013

concentrations of organic vapour above cloud base. Hence, strictly we can not assume that all of the organic vapour condensed onto the aerosol at cloud-base. However, because high updraft speeds and low aerosol numbers tend to result in high activated fractions the reduced condensed organic material appears to not factor significantly. This is because, even without the addition of organic material, nearly all of the aerosol activate at such high updraft speeds.

It is evident that the Fountoukis and Nenes (2005) scheme performs better in this comparison; however, at low updraft speeds it still underestimates the activated fraction when compared to the model. This effect happens more readily for high aerosol number concentrations. The reason for this is that at the point of activation the aerosol size distribution splits into those that remain interstitial and those that become activated into cloud drops. The large difference in size means that organic vapours will condense preferentially on to the largest particles in the size distribution, rather than be distributed equally over the whole size distribution, as we have assumed for the parameterisation. At present it is difficult to devise a way of overcoming this problem.

Parcel model simulations showed that the effect of condensation of organic vapours onto the aerosol size distribution served to increase the "dry" diameter of all particles by an approximately constant factor. This resulted in the arithmetic standard deviation remaining relatively constant and hence a reduction in the geometric standard deviation (as the geometric diameter increased). The physical basis for all sizes being increased by an approximately constant factor following co-condensation is that the true particle sizes are all quite similar as they consist mainly of water. This results in a constant diameter growth (see Appendix). Taking into account the fact that the arithmetic standard deviation did not change appreciably was crucial to accurately predicting the activated fraction (Sect. 2.2.2).

It is recognised that there may be other important factors to consider in such a parameterisation including: mass accommodation coefficients; entrainment rates and multiple aerosol modes (as was considered by Ghan et al., 2011). Nevertheless, owing to the fact that the parameterisations used are physically-based, such factors can be taken

ACPD
13, 14447–14475, 2013

into account in both representations. The additions derived herein that take in to account the effect of semi-volatiles do not prevent the inclusion of these effects.

5 Conclusions

A parameterisation for aerosol activation including semi-volatile co-condensation has been developed, for use in large-scale models, that carry representations organic vapour concentrations of different volatilities. It is based on the schemes described by Abdul-Razzak et al. (1998) and Fountoukis and Nenes (2005). The main addition is in the shifting of both the median diameter and the standard deviation of the non-volatile aerosol lognormal distribution. Although this paper presented calculations for a single lognormal mode, this can be extended to multiple lognormal modes as has been shown previously. One difficulty to overcome is how to partition the organic mass to each mode. This may be done in proportion to the total mass of each mode, since the theory shows that this is a main driving factor for co-condensation; however, this idea needs to be tested further.

The conclusions drawn from the study are as follows:

- Both the geometric diameter and the geometric standard deviation of the "effective dry" aerosol distribution shift during the co-condensation process. The reduction in geometric standard deviation is the main reason activated fraction increases (see Sect. 2.2.2).
- For the updrafts tested the inclusion of co-condensation results in a broadening of the distribution of activated fractions. It is evident that the Abdul-Razzak et al. (1998) implementation of the scheme significantly underestimates the mean activated fraction when compared to the parcel model and Fountoukis and Nenes (2005) scheme, especially when the effect of semi-volatiles is included.

ACPD
13, 14447–14475, 2013

– However, the Abdul-Razzak et al. (1998) scheme also seems to over-estimate the frequency of low activated fractions even without the inclusion of semi-volatiles (Fig. 8, green lines).

– It appears, at least for the conditions tested herein, that the Fountoukis and Nenes (2005) scheme performs better than the Abdul-Razzak et al. (1998) scheme when compared to the parcel model approach. This is especially evident at low updraft speeds (Figs. 4 and 5).

Appendix A

Why does the aerosol distribution not narrow with condensing organics?

To answer this question we assume the growth from the organic vapour of an aerosol particle that is an internal mixture of an involatile component and N semi-volatile components.

The well-known Maxwellian growth theory shows that such a particle will increase in diameter at a rate inversely proportional to its diameter:

$$\frac{\mathrm{d}d}{\mathrm{d}t} \propto \frac{1}{d} \tag{A1}$$

where d is the diameter of the particle. In the case of co-condensing organics it should be noted that, at the high humidities relevant for cloud formation, the particle consists mostly of water. Condensing water onto the particles results in a narrowing of the ratio of droplet diameters in a distribution (as predicted by both Maxwellian growth, $\frac{\mathrm{d}d}{\mathrm{d}t} \propto \frac{1}{d}$, and sub-saturated aerosol growth, $\frac{\mathrm{d}d}{\mathrm{d}t} \propto$ constant) and so near cloud base the droplet size distribution consists of a narrow ratio of droplet diameters.

The narrow distribution means we can approximate the term $\frac{1}{d}$ on the right-hand-side of Eq. (A1) to be a constant. Note that this is only the case for the condensing organics,

ACPD
13, 14447–14475, 2013

not condensing water vapour. In this situation we arrive at the result that, regardless of the initial particle size, the difference in particle size after co-condensation of organics is proportional to t. Therefore, if all particles experience the same growth time, their change in size will be a constant:

$$d_2 - d_1 \propto t \tag{A2}$$

where d_1 and d_2 are the initial and final particle diameters respectively. However, it should be noted that the diameters considered in Eqs. (A1) and (A2) are the true physical diameters of the drop, whereas for the parameterisation outlined in this paper we require the "dry" particle size. We now show, to a first approximation, that at cloud-base the "dry" particle size is directly related to the wet particle size.

Firstly we assume that, to a first approximation, the physical diameter is proportional to the cubed root of the sum of the number of moles of each component (strictly it actually the volume of the sum of each component). Therefore we can re-write Eq. (A2) as:

$$\left(n_c + n_{w,2} + \sum n_{i,2}\right)^{1/3} - \left(n_c + n_{w,1} + \sum n_{i,1}\right)^{1/3} \propto t \tag{A3}$$

where n_i is the number of moles of component i in the condensed phase; n_c is the number of moles of the involatile component (e.g. ammonium sulphate) and n_w is the number of moles of water. Raoult's law for water vapour in equilibrium at relative humidity, RH_{eq}, with an aerosol particle is:

$$RH_{eq} = \frac{n_w}{n_c + n_w + \sum n_i} \tag{A4}$$

which can be rearranged to make n_w the subject:

$$n_w = \frac{RH_{eq}}{1 - RH_{eq}} \left(n_c + \sum n_i\right) \tag{A5}$$

ACPD
13, 14447–14475, 2013

Hence, at equilibrium, the number of moles of water is proportional to the number of moles of all other components. Equation (A5) can then be substituted into Eq. (A3) with the result that the change in particle "dry" diameter is approximately constant for all sizes in the distribution.

Acknowledgements. This work was funded by the Natural Environment Research Council (NERC) Aerosol–Cloud Interactions – a Directed Programme to Reduce Uncertainty in Forcing (ACID-PRUF) programme, grant code NE/I020121/1. The Met. Office (Steve Abel) are acknowledged for providing the data for the PDF of updrafts in Fig. 7. A Fortran 90 code of the parameterisation described in the paper is available on request from the University of Manchester authors.

References

Abdul-Razzak, H., Ghan, S. J., and Rivera-Carpio, C.: A parameterization of aerosol activation. 1. Single aerosol type, J. Geophys. Res., 103, 6123–6131, 1998. 14449, 14452, 14453, 14458, 14459, 14460, 14462, 14463, 14471, 14475

Albrecht, B. A.: Aerosols, cloud microphysics and fractional cloudiness, Science, 245, 1227–1230, 1989. 14448

Cappa, C. D. and Jimenez, J. L.: Quantitative estimates of the volatility of ambient organic aerosol, 10, 5409–5424, 2010. 14454, 14457

Charlson, R. J., Lovelock, J. E., Andreae, M. O., and Warren, S. G.: Ocean phytoplankton, atmospheric sulphur, cloud albedo and climate, Nature, 326, 655–661, 1987. 14449

Fountoukis, C. and Nenes, A.: Continued development of a cloud droplet formation parameterization for global climate models, J. Geophys. Res., 110, D11212, doi:10.1029/2004JD005591, 2005. 14449, 14452, 14453, 14458, 14459, 14460, 14461, 14462, 14463, 14472, 14475

Ghan, S. J., Abdul-Razzak, H., Nenes, A., Ming, Y., Xiaohong, L., Ovchinnikov, M., Shipway, B., Meskhidze, N., Xu, J., and Shi, X.: Droplet nucleation: Physically-based parameterizations and comparative evaluation, Journal of Advances in Modeling Earth Systems, 3, M10001, doi:10.1029/2011MS000074, 2011. 14449, 14461

ACPD
13, 14447–14475, 2013

Kulmala, M., Suni, T., Lehtinen, K. E. J., Dal Maso, M., Boy, M., Reissell, A., Rannik, Ü., Aalto, P., Keronen, P., Hakola, H., Bäck, J., Hoffmann, T., Vesala, T., and Hari, P.: A new feedback mechanism linking forests, aerosols, and climate, Atmos. Chem. Phys., 4, 557–562, doi:10.5194/acp-4-557-2004, 2004. 14449

McFiggans, G., Topping, D. O., and Barley, M. H.: The sensitivity of secondary organic aerosol component partitioning to the predictions of component properties – Part 1: A systematic evaluation of some available estimation techniques, Atmos. Chem. Phys., 10, 10255–10272, doi:10.5194/acp-10-10255-2010, 2010. 14454

Solomon, S., Qin, D., Manning, M., Chen, Z., Marquis, M., Averyt, K. B., Tignor, M., and Miller, H. L.: IPCC, 2007: Climate Change 2007: The Physical Science Basis, Contribution of Working Group 1 to the Fourth Assessment Report of the Intergovernmental Panel on Climate Change, available at: http://www.ipcc.ch/pdf/assessment-report/ar4/wg1/ar4-wg1-spm.pdf, 2007. 14448

Topping, D. O. and McFiggans, G. B.: Tight coupling of particle size, number and composition in atmospheric cloud droplet activation, 12, 3253–3260, 2012. 14448

Topping, D. O., Connolly, P. J., and McFiggans, G. B.: Cloud droplet number enhanced by co-condensation of organic vapours, Nat. Geosci., doi:10.1038/NGEO1809, 2013. 14448, 14449, 14454, 14455, 14457

Twomey, S.: The nuclei of natural cloud formation: the supersaturation in natural clouds and the variation of cloud droplet concentration, Geofis pura et appl., 43, 243–249, 1959. 14453

Twomey, S.: The influence of pollution on the shortwave albedo of clouds, J. Atmos. Sci., 34, 1149–1152, 1977. 14448

vanZanten, M. C., Stevens, B. B., Nuijens, L., Siebesma, A. P., Ackermann, A. S., Burnet, F., Cheng, A., Couvreux, F., Jiang, H., Khairoutdinov, M., Kogan, Y. L., Lewellen, D. C., Mechem, D., Nakamura, K., Noda, A., Shipway, B. J., Slawinska, J., Wang, S., and Wyszogrodzki, A.: Controls on precipitation and cloudiness in simulations of trade-wind cumulus as observed during RICO, Journal of Advances in Modeling Earth Systems, 3, M060001, doi:10.1029/2011MS000056, 2011. 14459

ACPD
13, 14447–14475, 2013

Table 1. Nomeclature.

n_{ap}	Number of aerosols per unit volume, per logarithmic interval, page 4
N_{ap}	Total number of particles per unit volume, page 4
d_{ap}	Particle diameter, page 4
d_m	Median particle diameter, page 4
$\ln\sigma$	Standard deviation of $\ln\frac{d_{ap}}{d_m}$, page 4
S_{crit}	Critical supersaturation of an aerosol diameter d_{ap}, page 4
$S_{c,\,m}$	Critical supersaturation of an aerosol with diameter equal to d_m, page 4
$e_{sat,\,l}$	Saturation vapour pressure over liquid water, page 4
S_l	Supersaturation over liquid water, page 4
e	Vapour pressure of water, page 4
$e_{sat,\,l}$	Saturation vapour pressure over liquid water, page 4
w_v	Water vapour mixing ratio, page 5
P	Pressure, page 5
T	Temperature, page 5
R_v	Specific gas constant for water vapour, page 5
L_v	Latent heat of vapourisation, page 5
R_a	Specific gas constant for air, page 5
c_p	Specific heat capacity of air, page 5
w_l	Liquid water mixing ratio, page 5
w_i	Ice water mixing ratio, page 5
L_s	Latent heat of sublimation, page 5
w	Ascent velocity of parcel, page 5
g	Gravitational field strength, page 5
R_a	Specific gas constant for air, page 5
d	Diameter of a drop, page 6
G	Thermodynamic factor, page 6
m	Mass of a drop, page 6
ρ_w	Density of liquid water, page 6
d_1	initial diameter of particle, page 18
d_2	final diameter of particle, page 18
n_i	Number of moles of component i in the condensed phase, page 18
n_c	Number of moles of involatile component, page 18
n_w	Number of moles of condensed water, page 18
RH_{eq}	Equilibrium relative humidity, page 18

ACPD
13, 14447–14475, 2013

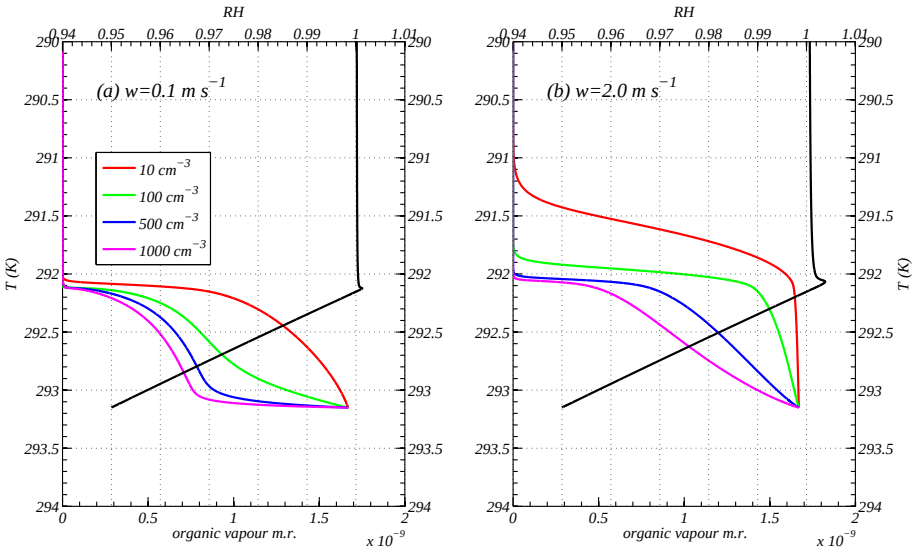

Fig. 1. (a) shows the organic vapour content in the parcel plotted against temperature (coloured lines) for parcel model simulations assuming an updraft speed of 0.1 m s^{-1}. The different coloured lines correspond to parcel model simulations that contain different total aerosol number concentrations (as in the legend). The black line is the humidity for the simulation with 1000 cm^{-3} aerosol particles. **(b)** is as for **(a)**, but for an updraft velocity of 2.0 m s^{-1}.

ACPD
13, 14447–14475, 2013

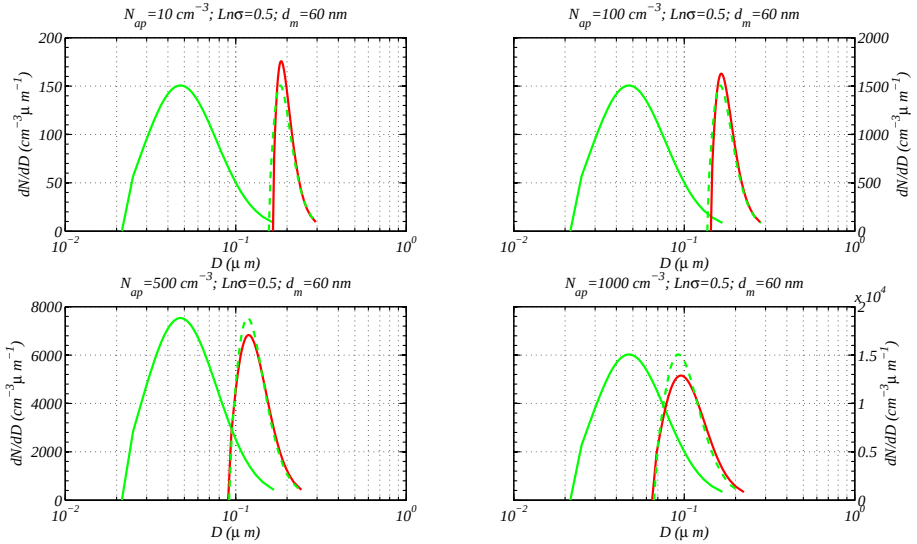

Fig. 2. Particle size distributions before and after co-condensation at 95 % RH. Top left is for total aerosol concentration of 10 cm^{-3}; top right is for 100 cm^{-3}; bottom left is for 500 cm^{-3} and bottom right for 1000 cm^{-3}. The green solid line is the non-volatile aerosol particle distribution, whereas the red solid line is the aerosol particle distribution after co-condensation of semi-volatiles (this excludes the liquid water so is only the effective "dry" aerosol size). The green dashed line is the original non-volatile distribution that has been shifted in diameter space by a constant factor. These aerosol size distributions are plotted on a logarithmic scale for the diameter.

ACPD
13, 14447–14475, 2013

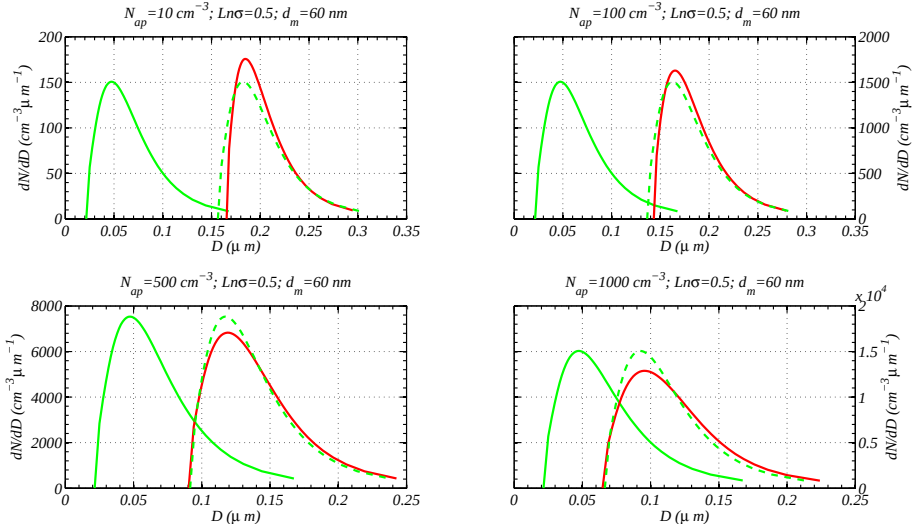

Fig. 3. Same as Fig. 2 but plotted on a linear scale for the diameter.

ACPD
13, 14447–14475, 2013

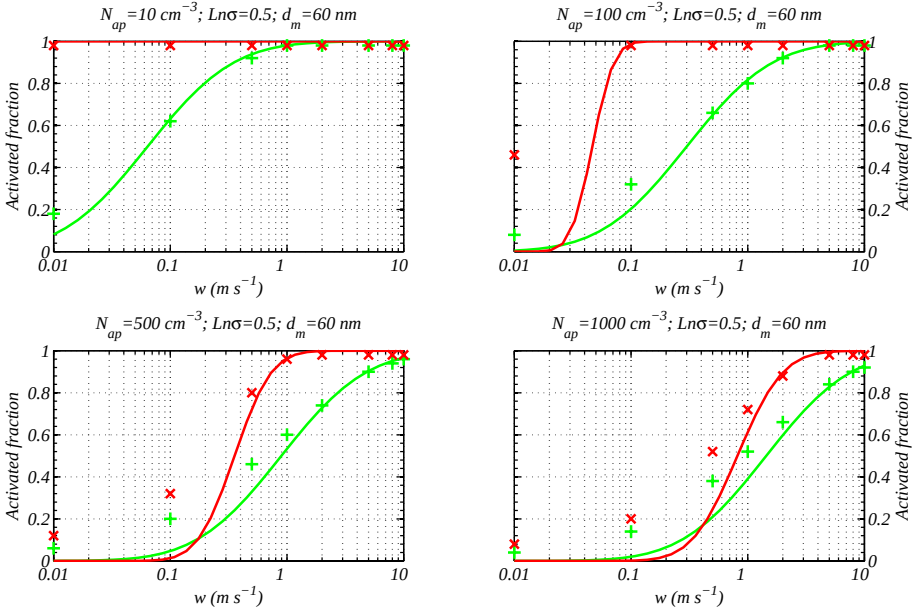

Fig. 4. Comparison of the parcel model with the Abdul-Razzak et al. (1998) implementation for both with and without semi-volatile co-condensation. Top left is for 10 cm^{-3} total aerosol; top right is for 100 cm^{-3}; bottom left is 500 cm^{-3} and bottom right is for 1000 cm^{-3}. Crosses are the parcel model results and solid lines are the parameterisation. Green lines for without semi-volatile condensation and red with.

ACPD
13, 14447–14475, 2013

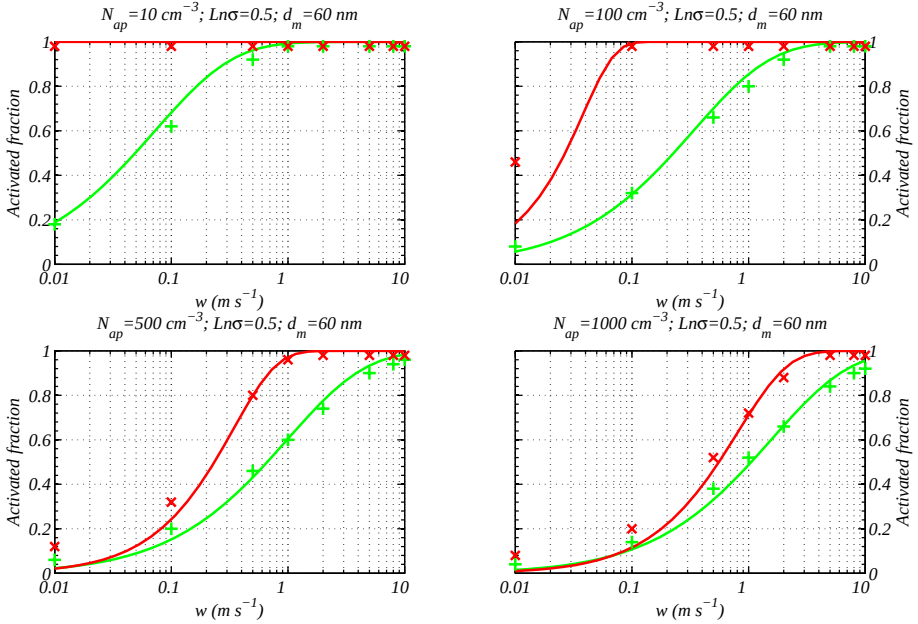

Fig. 5. Same as Fig. 4 but for the Fountoukis and Nenes (2005) implementation.

ACPD
13, 14447–14475, 2013

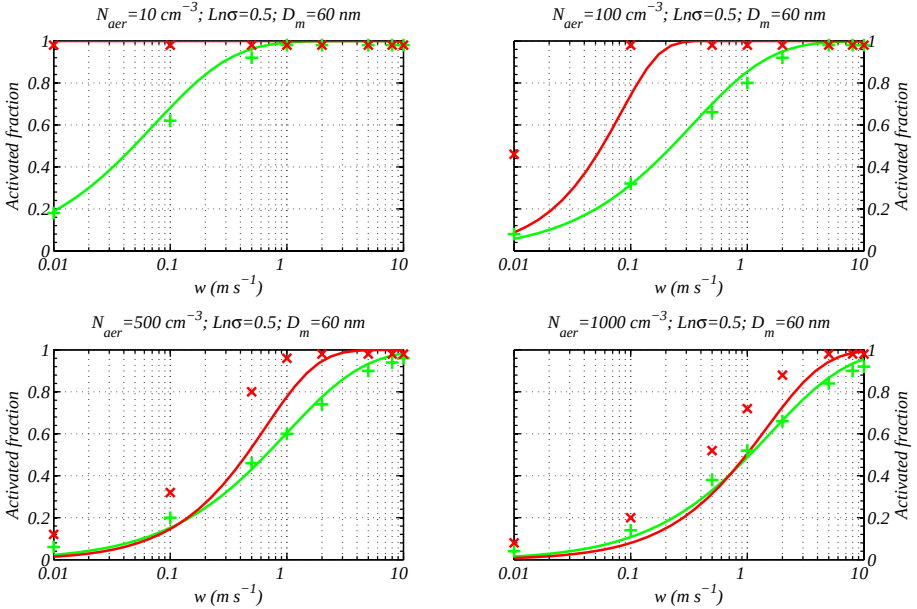

Fig. 6. Same as Fig. 5 but without shifting the geometric standard deviation, lnσ.

ACPD
13, 14447–14475, 2013

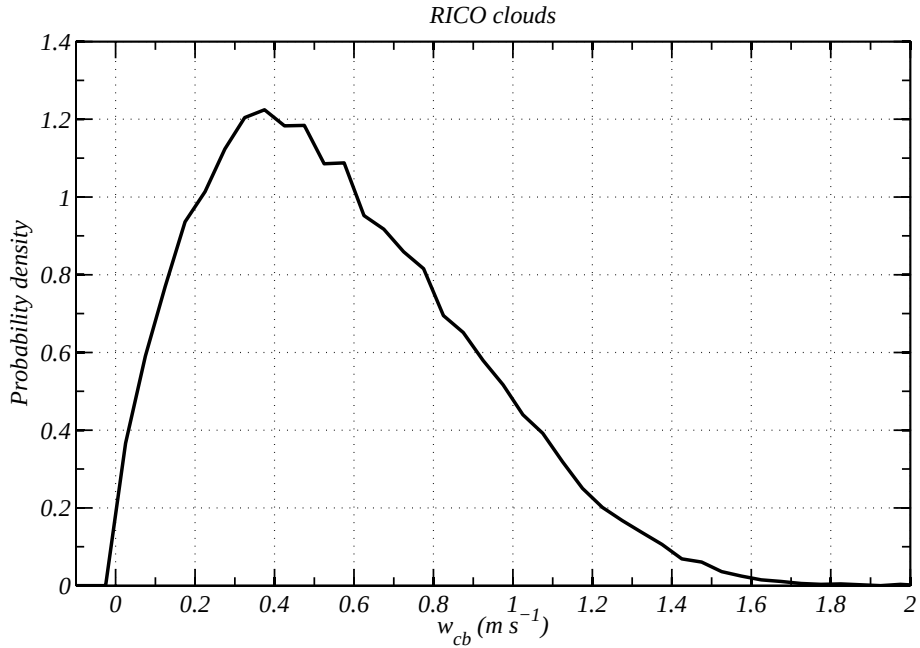

Fig. 7. The PDF of updraft velocities derived from Rain In Cumulus over the Oceans (RICO). This is presented as a probability density, where $\int_0^\infty P \mathrm{d}w_{\mathrm{cb}} = 1$.

ACPD
13, 14447–14475, 2013

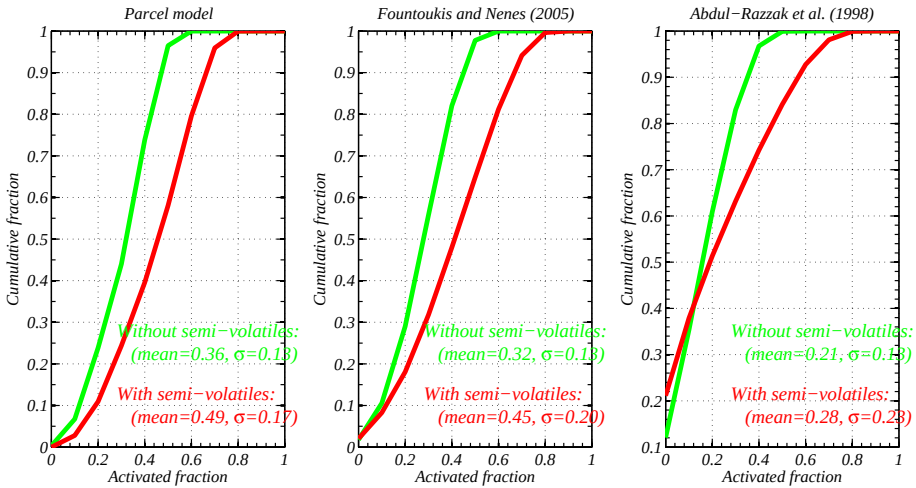

Fig. 8. Cumulative frequency of activated fraction for: parcel model simulations (left); Fountoukis and Nenes (2005) implementation (centre); Abdul-Razzak et al. (1998) implementation (right). Green is without semi-volatile co-condensation; red is with.

ACPD
13, 14447–14475, 2013